Long-Short Gamma Ray Bursts Energy Spectra Analysis*

Vytis Krupovnickas†
Columbia University

Gamma ray bursts (GRBs) are relatively brief energetic phenomena characterized by intense gamma radiation. GRBs are divided into long and short categories based on their duration. Long GRBs are believed to largely stem from the death of a star through a supernovae explosion. Short GRBs are theorized to be due to the merger of two compact objects, such as neutron stars or black holes. A third class of GRB can be described as having high energy properties but containing kilonova associations related to the merger of compact objects. GRB 211211A was a long duration short gamma ray burst of this third category detected in December 21, 2021. Its prominent kilonova association provides compelling evidence that this GRB was the result of a compact merger. GRB 230307A was another long short GRB which had a similar burst pattern to GRB 211211A. The similarities between the GRBs - namely, a precursor followed by two prominent peaks and three weaker and smaller peaks - prompt investigation into whether previous events can be found in the Fermi catalogue. Using the data provided by NASA's Fermi Gamma Ray Space Telescope, we investigate the energy spectrum of GRB 211211A and related long duration short gamma ray bursts with kilonova associations to characterize properties within the events which might give insight into the nature of these types of GRBs. Using machine learning methods we hope to develop a method for finding events which have similar characteristics to the known long-short GRBs. We anticipate that our results will be useful for further investigations in long-short GRBs, which can can aid in our understanding of neutron star geography as well as expand multi-messenger astronomy.

I. INTRODUCTION

During the collapse of massive stars or merger of compact objects, such as neutron stars or black holes, energy is released in the form of a gamma-ray burst (GRB), a powerful and brief release of gamma-ray radiation. The photons released from GRBs takes on a broad energy spectrum, ranging from visible light to gamma and x-rays, all of which are important in studying these astrological phenomena. The visible light released from GRBs make them some of the brightest events in their galaxies for brief periods of time, which is useful to cosmologists as a standard candle for measuring distances in the universe. The ultraviolet and infrared portions of the spectra can elucidate the nature of the event as well as its origins, being the regime where kilonova signatures are often detected. GRBs give insight into the nature of compact object mergers when combined with other astronomical events, such as gravitational waves and high-energy cosmic rays, which can aid in understanding the universe through multi-messenger astronomy.

Kilo-novae, another important component of analyzing GRB data, are transient astronomical events that can follow GRBs, resulting from the ejection of heavy neutron-rich material during the merger of neutron stars. These kilonovae produce visible and infrared signatures, including a rapid and short-lived increase in brightness, and the production of heavy elements like gold and platinum through rapid neutron capture (r-process) nucleosynthesis, which can be detected through spectroscopic analysis. Studying the connection between GRBs and kilo-novae offers valuable insights into the astrophysical processes associated with these high-energy phenomena and the origin of heavy elements in the universe.

GRBs can be broadly divided into two major categories: short GRBs, which last under two seconds, sometimes only milliseconds, and long GRBs, which last for two minutes or more. Long GRBs compose nearly 70% of all detected events, whereas short GRBS compose 30%. Short bursts tend to be ten times dimmer than long bursts, and consist of more energetic gamma rays. There is some speculation about the origin of short and long GRBs, although there is conclusive evidence that many long GRBs come from hyper-nova explosions. Short GRBs are believed to arise from neutron star mergers, although their origins are enigmatic.

In this study we examine long GRBs with associated kilo-novae signatures and gravitational waves. The GRBs we seek to investigate in detail are high energy long GRBs which showed count rates two magnitudes higher than the background, producing distinct peaks (illustrated in figure) whose energy signatures may hold something of significance, prompting further study into different aspects of the GRB data.

II. METHODOLOGY AND DESCRIPTION

A. Fermi Gamma Ray Space Telescope

The Fermi Gamma Ray Space Telescope was an initiative by NASA launched on June 11, 2008 by the Delta

* Performed in Marka Laboratory
† Also at Physics Department, Columbia University.

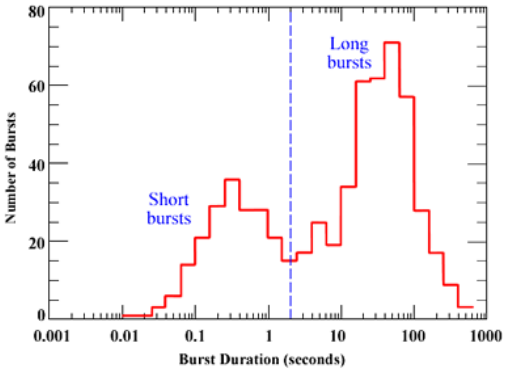

FIG. 1. Histogram of quantity of short bursts and long bursts showing duration for events within each bin. Taken from astronomy.swin.edu.au

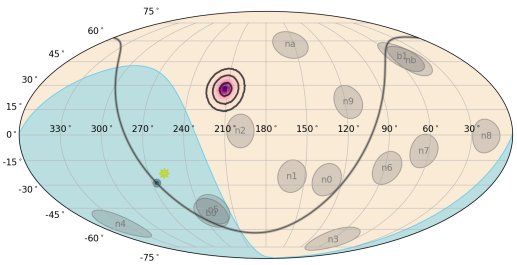

FIG. 2. GRB 211211A skymap, showing localization of event in region of sky Fermi Gamma Ray Telescope was pointed at during detection.

7920H rocket to investigate cosmic ray signals. All event times are measured from this date, the mission start date. The telescope orbits Earth at an altitude of 535 km in an oscillating pattern so that it can obtain a full measurement of the sky every three hours. The detector contains two bismuth germanate (BGO) scintillation crystals (b0, b1) and twelve sodium iodide (NaI) scintillation crystals (na, nb, n0-9). These crystals are pointed normal to each other as shown in Figure 2. This configuration gives the telescope a full range of not just the sky but also of the Earth, allowing for detection of Earth occlusion events.

The crystal detectors within the telescope detect events in different directions and at different energy sensitivities. The BGO crystal is a 12.7 cm cylinder installed on either ends of the cube. Two of these are placed on opposite sides of the monitor, and have two PMT coupled to either end for each crystal to allow for better light collection. The BGO crystal detects energy in the range 200 keV to 40 MeV, which encapsulates the energy range between the sodium iodide detectors and Fermi LAT (Large Area Telescope). The NaI detector has the same dimensions as the BGO crystal and is placed on the corners of the cube to give it a full range outside of the range occulted by Earth. The NaI detectors are enclosed in a Beryllium window which enables the crystals

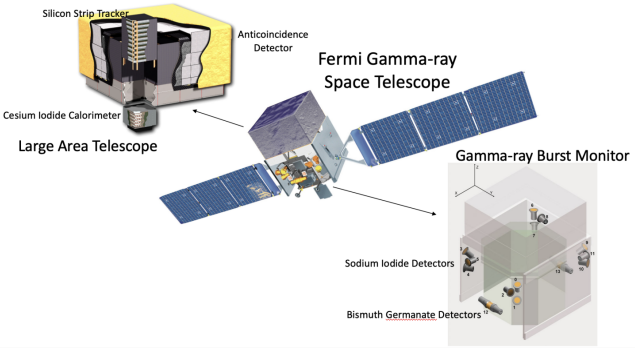

FIG. 3. Fermi Gamma Ray Space Telescope scintillation crystals housing unit, as well as configuration of crystals. The telescope contains fourteen crystals, twelve NaI and two BGO detectors. Crystals are pointed normal to each other, with the BGO detectors on either side of unit.

to detect photons in the 8 keV to 1 MeV energy range. The crystals are calibrated according to the LAT Light Curve Repository (LCR), which consists of a database of variable light curves over 1500 sources.

III. DATA ANALYSIS

A. Method

The data is obtained using Fermi GBM Data Tools available on the NASA Fermi website, which contains methods and functions for downloading the files, plotting the data, looking at the energy spectra, and taking the raw data from the files to further process for data analysis. Signals are processed by an onboard digital processing unit and digitized into 4096 energy channels. Signals above a certain threshold are converted into 128 energy channel and 8 energy channel data types for further analysis. The information is automatically binned in the CSPEC and CTIME files, and unbinned time-tagged events (TTE) files are available for all events since 2012.

The CSPEC data consists of 128 energy channel bins with a default time resolution of 4.096s. The CTIME data consists of 8 energy channels with a default resolution of 256ms. The TTE (time-tagged events) data file consists of 128 energy channels, 2μs time resolution, and associated detector identification for events. The CSPEC data, due to its low binning resolution, was most useful for peak identification and analysis, with the CTIME data having little use past a broad overview of the background event data. The TTE data was most useful for data analysis, as it contained the highest resolution raw data and could be easily binned to coarser time bins.

The TTE data for each detector was binned with a resolution of 0.2s, as this provided the best view of the energy spectra for the events without suffering too heavily from artefacts created through the instrumentation. The data primitives contained methods through which

the energy centroids, time centroids, and counts could be easily obtained. The count data consisted of a 2D array, displaying the number of count events per energy channel for that time bin. This data was used to create a spectral count heat map showing the frequency of events at their energy bins for that time. For every detector the total counts were summed and used to create a series of spectral heat maps showing the data for the NaI and BGO detectors, which capture the full energy range of the event.

IV. RESULTS

A. Lightcurves for GRB 211211A and GRB 230307A

The lightcurves for the events present a quick way to see the major spectral features of the GRBs. A lightcurve will show count rate in units of counts/s versus the time of the event. The lightcurve will have background bins of 8.124s from the start of the trigger event to time zero, then to around 50s after after the trigger time through the rest of the data. Between these two background bins, there are 1.024 s duration bins, and in a very short window around the trigger time, there are overlapping bins of width 256 and 64 ms. The lightcurve was intended to give a quick look at the event and acts as a good starting point for analyzing an event. The peaks represent the total counts which were recorded for that time frame, giving a quick over view of the characteristics of the event, such as strength, duration, and count rate for the peaks. For each event there are several distinct peaks over a significant time frame, which allow us to characterize the GRB as either short or long but especially get a perspective into the shape of the event. Some events of precursors which appear in the negative time range and can be significant for understanding the engine behind the event.

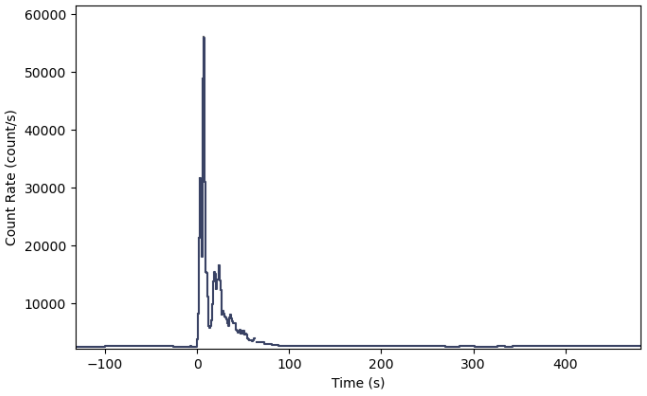

FIG. 4. The light curve of long GRB 211211A shows five major peaks.

We investigate the energy spectra for the duration of the event to see if there is anything significant in the spectrum. To do this, we can use the $'.to_spectrum()'$ method to obtain the energy regime for the t90 duration of the event (the time after t_0 for which 90% of the event flourescence occurs). An example of this is given in Figure 8, and when the event centroids are normalized using the following equation:

$$x_n = \frac{x - x_{min}}{x_{max} - x_{min}} \tag{1}$$

Which is graphed in Figure 7.

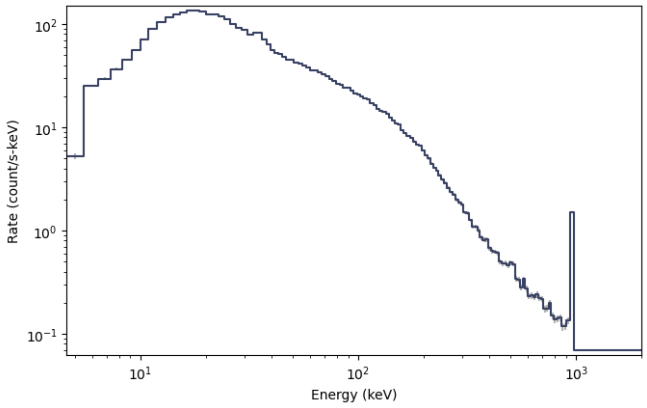

FIG. 6. The energy spectrum for GRB 211211A. The energy is given in keV and the rate is given in counts/s*keV. Not that there are 128 bins, with the last two bins containing the upper edges of the NaI detector's sensitivity, which "spill over" into the BGO detector. These can be truncated from the data during the background cleaning.

From these normalized spectra we observe that for many events there exists two hills of energy at the beginning of the event, which decrease until reaching the upper edge of the detector's energy sensitivity range. The Fermi

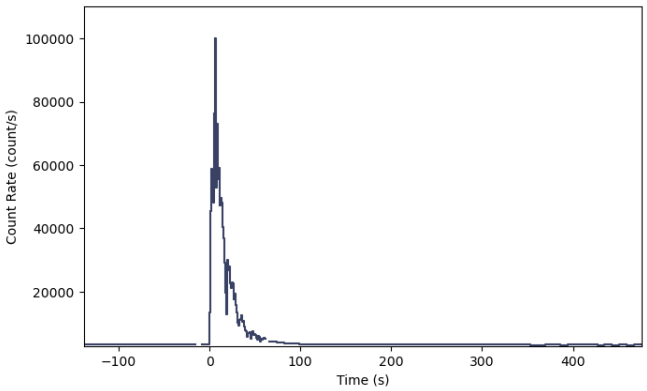

FIG. 5. The light curve of long GRB 230307A shows five major peaks with the same descending power curve behind the events, and a feint but rising peak following the main engine of the event.

software compresses all events at the edge of its range into one bin which skews the counts for lower-energy detectors, but is given a finer resolution for the BGO detector, which is not included in this graph. Short GRBs will have a spectrum with far more variation, which will decreases more rapidly.

The energy spectra for the peaks of GRB 211211A are normalized and graphed against each other as shown in Figure 8. These peaks were analyzed against each other to investigate differences in the spectra, and see if anything can be observed within their regimes. The peaks tend to coincidence with the total counts within their event duration, and thus nothing significant could be determined from their normalized spectra.

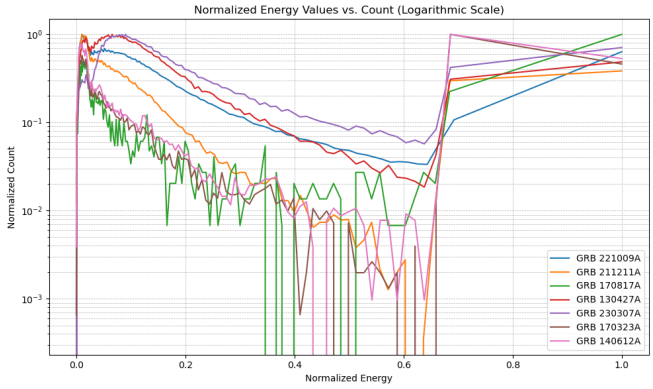

FIG. 7. The energy spectra for the full duration of the events for several GRBs, both long and short, are normalized and graphed against each other. Long GRBs generally have a double hill features at low energies which are not present with kilonova associated GRBs.

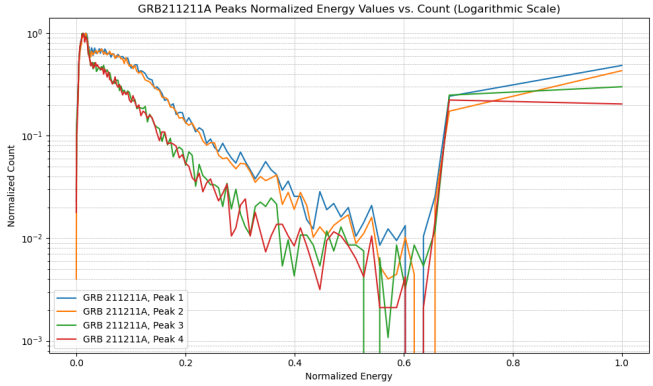

FIG. 8. For each significant peak in GRB 211211A, the energy spectra for the duration of the event was normalized and graphed against the other peaks.

The lightcurve, although visually useful for determining the form and length of an event, does not have much use in the way of analyzing the event. Thus, in order to construct a more visually and analytically useful structure for the event, one which allows us to understand the energy, counts, and time factors of the event, we need to look at the time-tagged event (or TTE) files.

The TTE files include useful metadata and extensions which allow us to manipulate the data and bin it in ways which are useful for analyzing the data. The TTE file extension '.data' allows one to get the 'EventList' objects from the event, from which we can bin the data and extract the counts, time, and energy data for the event. The counts are represented as a 2D array with dimensions equal to the size of the times and energy centroid arrays, which can be plotted in a sort of spectrogram which we term a count heat map. For both the BGO and NaI event there are 128 energy bins, although the centroids of these bins vary for each event. These attributes can then be graphed in Python using the 'mathplotlib' library in an 'imshow' plot, as shown in Figures 9 and 10. We use the 'cmap' 'viridis' color scheme to more easily see the fine structure of the event.

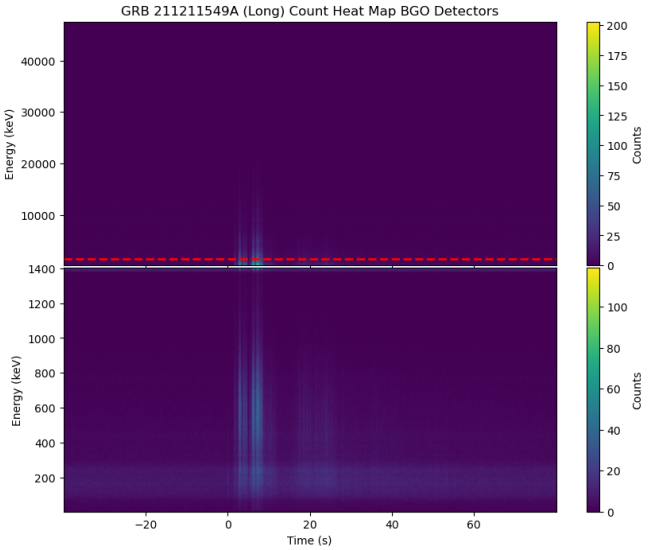

FIG. 9. The "count heat map" of the long-short GRB 211211A. The BGO detectors are shown in the top graph, the NaI detectors shown in the botom graph. The counts for all bins are summed and then plotted to form the heat map for the entire event. The dotted red line on the top graph represents the max energy bin for the NaI detectors, demarcating the regime in which higher energy values are detected for the event. Note the linear background around the 200 keV energy range.

The energy range calibration for the detectors is graphed on the y-axis, the time on the x-axis, and the counts per energy bin graphed at the centroid for each time bin where greater quantities are attributed to a brighter color. These spectral heat maps show the energy and quantity of photons for each event, which gives valuable insight into the energy of the burst.

In order to see the fine structure of the event, and for shorter GRBs see the fine structure for their events, it is necessary to remove the background.

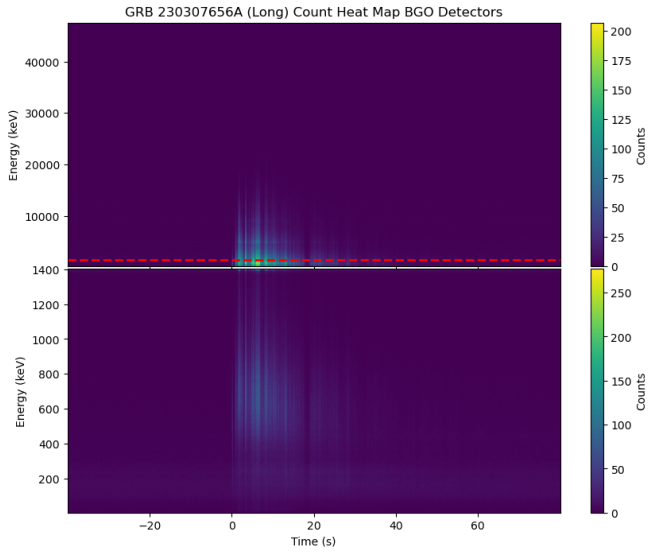

FIG. 10. The count heat map of GRB 230307A shows similar features to the heat map of GRB 211211A, although it is necessary to remove the background to see the major features of the event.

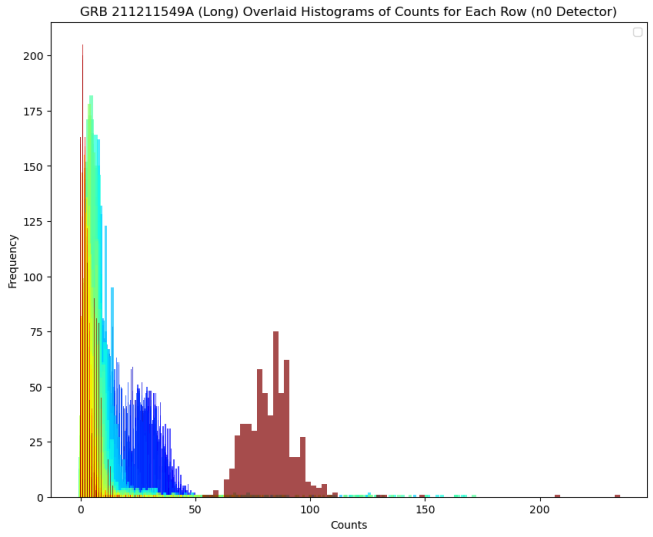

FIG. 11. Histogram of counts by energy bin for event GRB 211211A. The colors scale from light blue to dark red based on the value of the energy bin, with light blue colors representing lower energy bins and dark red representing higher energy bins, Note the block of red representing the last two bins in the histogram.

B. Removing the Background

The background is contributed by several different sources depending on the detector direction during the duration of the event. These consist of everything from cosmic background radiation to radiation from the sun and Earth to large storms on Earth, some of which emit gamma rays. Electrical noise is another factor which must be filtered out using alternative methods, as it follows a random pattern thus making it difficult to remove with mean or histogram methods.

Additionally, due to the movement of the satelitte during the duration of longer events - as well as other contributing factors - the background can take on a nonlinear form. As a result, an algorithm must be designed to find the mean of the background for each energy bin, which is then matched to the total form of the bins and subtracted from the graph for each bin. Then, a histogram is assembled for all the bins. An example is shown in Figure 10, showing the histogram of bins for GRB 211211A. The event is contained in the tail of the histogram, so in order to further remove the background, the lower 90th percentile of the event is truncated from the graph.

The bins are smoothed with a smearing factor to prevent edge effects from mapping the counts to the bin centroids, to highlight the form of the event. The top most rows of the NaI detectors (the first and second highest bins) are removed as they contain no useful information, and detract from the major event features. A median filter is used to remove the "salt and pepper" noise to further highlight the event. This works by taking the mean of the indices of radius three from the selected index and setting that count to the mean. Finally, the counts are normalized and then plotted logarithmically to better see the fine structure of the event. Additionally, the trigdat file gives a list of detectors in which the event was detected, which makes it significantly easier to filter bins in which the event has a detectable signature. The final results for GRB 211211A is shown in figure 13.

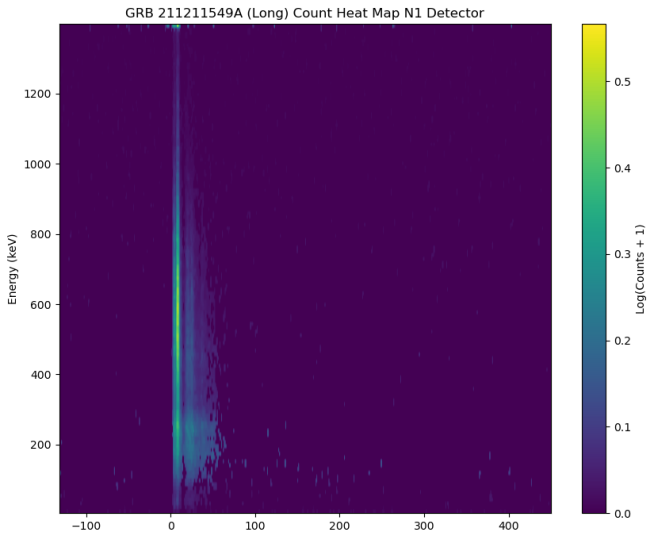

FIG. 12. Elimination of the background for the NaI detectors through the methods described. The event is far more visible and the form of the event is more easily determined.

V. PIPELINE

For the purposes of assembling a sizeable database to index from, a pipeline was constructed to create a set of count heat maps for the time ranges -15s to 15s; -50s to 50s; and 150s to 150s to capture short and logn GRBs, and the fine structure for long GRBs. The count heat maps were created with bin width 1.024s to fully capture both long and short GRBs. A set of these GRBs is shown in the appendix. See our GitHub repository for the code [1].

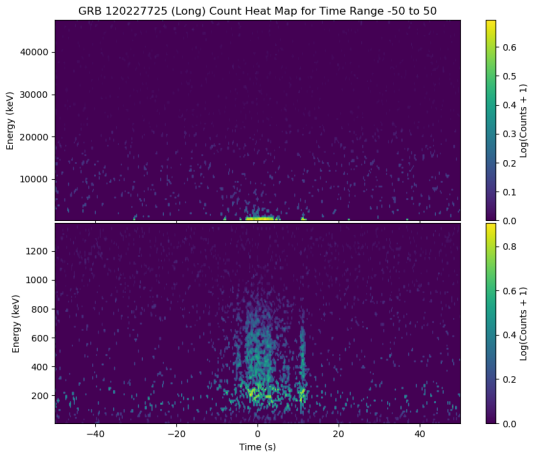

FIG. 13. GRB 120227A

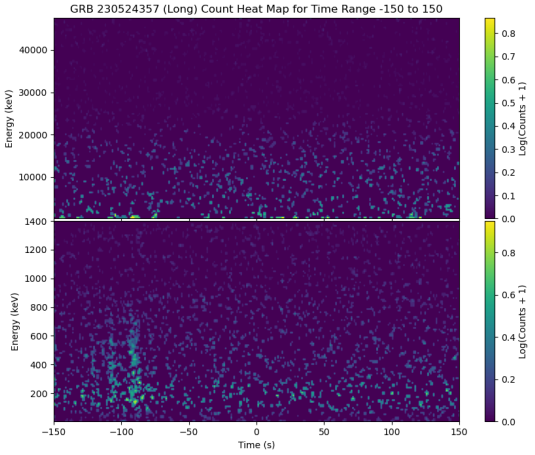

FIG. 14. GRB 230524A

---

[1] Vytis Krupovnickas. Long-short-grb-pipeline. `https://github.com/Vytis-K/Long-Short-GRB-Pipeline`, 2024. GitHub repository.

Appendix A: References

The quasi-periodically oscillating precursor of a long gamma-ray burst from a binary neutron star merger

Evidence for two distinct populations of kilonova-associated Gamma Ray Bursts

A luminous precursor in the extremely bright GRB 230307A

Fermi Gamma-ray Space Telescope, David J. Thompson and Colleen A. Wilson-Hodge

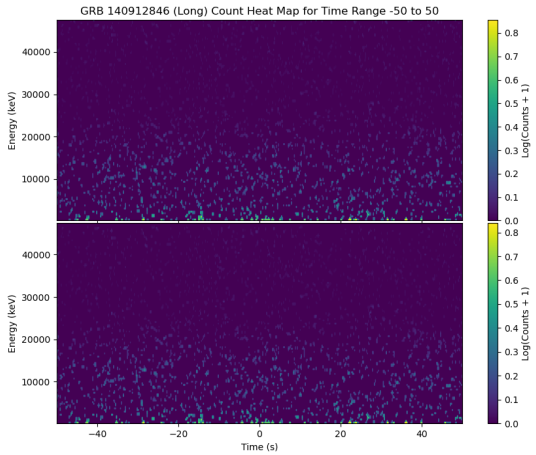

FIG. 15. GRB 140912A

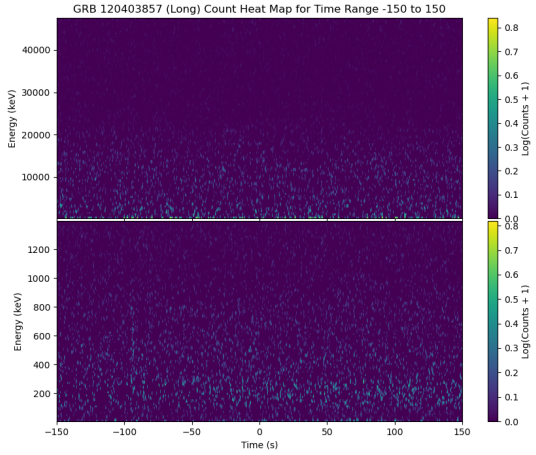

FIG. 16. GRB 120403A